

Undersampling power-law size distributions: effect on the assessment of extreme natural hazards

Eric L. Geist & Tom Parsons

Natural Hazards

Journal of the International Society
for the Prevention and Mitigation of
Natural Hazards

ISSN 0921-030X

Nat Hazards

DOI 10.1007/s11069-013-1024-0



Your article is protected by copyright and all rights are held exclusively by US Government. This e-offprint is for personal use only and shall not be self-archived in electronic repositories. If you wish to self-archive your article, please use the accepted manuscript version for posting on your own website. You may further deposit the accepted manuscript version in any repository, provided it is only made publicly available 12 months after official publication or later and provided acknowledgement is given to the original source of publication and a link is inserted to the published article on Springer's website. The link must be accompanied by the following text: "The final publication is available at link.springer.com".

Undersampling power-law size distributions: effect on the assessment of extreme natural hazards

Eric L. Geist · Tom Parsons

Received: 12 July 2013 / Accepted: 27 December 2013
© US Government 2014

Abstract The effect of undersampling on estimating the size of extreme natural hazards from historical data is examined. Tests using synthetic catalogs indicate that the tail of an empirical size distribution sampled from a pure Pareto probability distribution can range from having one-to-several unusually large events to appearing depleted, relative to the parent distribution. Both of these effects are artifacts caused by limited catalog length. It is more difficult to diagnose the artificially depleted empirical distributions, since one expects that a pure Pareto distribution is physically limited in some way. Using maximum-likelihood methods and the method of moments, we estimate the power-law exponent and the corner size parameter of tapered Pareto distributions for several natural hazard examples: tsunamis, floods, and earthquakes. Each of these examples has varying catalog lengths and measurement thresholds, relative to the largest event sizes. In many cases where there are only several orders of magnitude between the measurement threshold and the largest events, joint two-parameter estimation techniques are necessary to account for estimation dependence between the power-law scaling exponent and the corner size parameter. Results indicate that whereas the corner size parameter of a tapered Pareto distribution can be estimated, its upper confidence bound cannot be determined and the estimate itself is often unstable with time. Correspondingly, one cannot statistically reject a pure Pareto null hypothesis using natural hazard catalog data. Although physical limits to the hazard source size and attenuation mechanisms from source to site constrain the maximum hazard size, historical data alone often cannot reliably determine the corner size parameter. Probabilistic assessments incorporating theoretical constraints on source size and propagation effects are preferred over deterministic assessments of extreme natural hazards based on historical data.

Keywords Extreme natural hazards · Catalog · Empirical · Power law · Undersampling · Pareto · Probability

E. L. Geist (✉) · T. Parsons
U.S. Geological Survey, 345 Middlefield Rd., MS 999, Menlo Park, CA 94025, USA
e-mail: egeist@usgs.gov

1 Introduction

There have been several recent cases of natural hazards that were unexpectedly large relative to the results of prior hazard models. The most obvious example is the 2011 Tohoku-oki earthquake and tsunami, both of which exceeded expectations based largely on historical precedent (cf. Rikitake and Aida 1988; Stein et al. 2012). The 2004 Sumatra–Andaman earthquake and accompanying tsunami were also unexpectedly large for this region, with the latter producing devastating consequences. Large floods such as the 1993 Mississippi River and 2006 Danube River floods, which exceeded historical maximum water levels (cf., Malamud et al. 1996; Mikhailov et al. 2008), conform more to a power-law-type (Pareto) size distribution with a heavier tail than conventionally used distributions.

There is a wealth of both geophysical and statistical literature indicating that many natural hazards follow a power-law distribution of sizes. Earthquakes are perhaps the most well-known hazard that can be described by a power law. Early studies on earthquakes (Ishimoto and Iida 1939; Gutenberg and Richter 1944) indicated a power-law decay of size, i.e., a linear relationship on a semilog plot between earthquake magnitude (m) and the total number of events $\geq m$. The primary observed hazard effects of earthquakes, such as ground acceleration and/or seismic intensity, are complicated by earth structure, leading to variable attenuation, seismic ray path distortion, and frequency-dependent amplitude losses; thus, the ground-shaking hazard in the most important frequency bands can saturate, or not wholly depend on earthquake magnitude (Andrews et al. 2007). Other effects of earthquakes such as tsunami generation do not appear to exhibit saturation (Geist 2012).

More recent studies have indicated that other solid-earth natural hazards such as rock falls and landslides also appear to exhibit power-law behavior (Hergarten and Neugebauer 1998; Dussauge et al. 2003; Malamud et al. 2004; ten Brink et al. 2006). The sizes of hydrologic hazards such as riverine flooding (measured by discharge) and tsunami flooding (measured by run-up) follow a power-law decay, as indicated by, for example, Turcotte and Green (1993) and Burroughs and Tebbens (2005), respectively. The power-law relation also extends to wildfires (Strauss et al. 1989; Malamud et al. 1998; Cumming 2001; Schoenberg et al. 2003), volcanic eruptions (Mason et al. 2004), snow avalanches (Birkeland and Landry 2002), and solar flares (Lu and Hamilton 1991). The specific probability distribution used to describe these phenomena is termed a Pareto distribution, which exhibits a power-law decay of sizes above a minimum threshold size. Statistical tests of whether a Pareto or some other distribution best describes the tail of a given empirical distribution are discussed by, for example, Clauset et al. (2009).

Upper limits to the power-law relation have been difficult to quantify. Each natural hazard likely has a physical limit, for example the size of a drainage basin or the area of a fault that an earthquake can occur on. In many cases, however, the upper limit has been severely underestimated by historical data. We demonstrate this effect by estimating the parameters of a tapered Pareto distribution using historical catalog data for different natural hazards. The tapered Pareto distribution applies an exponential taper to the Pareto cumulative distribution. This taper is generally thought to be consistent with the behavior of dissipative physical systems (Kagan 1993) and mixing different truncated Pareto distributions (e.g., earthquake magnitude distributions on different faults) (Sornette et al. 1991). Further, physical justification for tapered Pareto distributions is described by Sornette and Sornette (1999) and Vere-Jones et al. (2001). Alternate modifications to the Pareto distribution for large sizes include tapering the Pareto density distribution with an

exponential function (termed a gamma distribution by Kagan 2002) (Kagan 1993; Main 1996; Sornette and Sornette 1999) and sharp truncation at a maximum size (Utsu 1999; Kagan 2002). For the latter, Kijko and Graham (1998) and Kijko (2004) provide statistical methods to determine the truncation point from the catalog data. Pisarenko and Sornette (2004) determine the crossover point between a generalized Pareto distribution and either an exponential or power-law taper, both of which result in a steeper decay of the distribution functions. Finally, Chakrabarty and Samorodnitsky (2012) recently discuss statistical tests to generally discriminate between tapered and truncated Pareto distributions.

The objective of this study is to characterize the effect of undersampling natural hazards that tend to follow power-law scaling. This includes diagnosing artificial tail shapes caused by finite sampling from historical catalogs that have previously and commonly been attached physical significance in hazard models. The undersampling problem has recently been discussed for earthquakes by Holschneider et al. (2011) and Zöller (2013) from a Bayesian perspective. The objective of this study is to also apply quantitative parameter estimation techniques to a variety of natural hazards. Estimation of the size distribution tail is important for natural hazard assessments, as the extreme event sizes can often dictate the overall hazard and necessary degree of preparedness (Strauss et al. 1989; Hergarten 2004; Sornette 2004), as well as catastrophic insured losses (Kagan 2007).

In this study, we demonstrate the effects of undersampling Pareto distributions on extreme natural hazards as follows. In Sect. 2, the properties of the Pareto and tapered Pareto distributions are described, as well as parameter estimation techniques and methods to generate synthetic catalogs. Several tests using synthetic catalogs are described, varying the catalog size and corner size parameter relative to the measurement threshold. These techniques and findings are applied to three types of natural hazards in Sect. 3: tsunamis, floods, and earthquakes. Examples were chosen that have a sufficient catalog length and that have special significance, such as the 2011 Tohoku-oki tsunami and stream gauge records from different climate regions. Finally, in Sect. 4, we discuss general implications of undersampling for future hazard assessments. Results of this study provide guidance on using historical catalog data as a basis for estimating extreme hazards.

2 Estimating and sampling Pareto and tapered Pareto distributions

2.1 Distribution functions

The cumulative and density functions of the Pareto and tapered Pareto probability distributions are defined below. Both distributions include an observational threshold parameter A_t . A_t may also be specified as the smallest value for which power-law behavior holds (Newman 2005). The cumulative number of events with event-maximum amplitude greater than A is given by

$$\Phi(A) = \left(\frac{A_t}{A}\right)^\beta \quad \text{for } A_t \leq A, \quad (1)$$

where β is the shape parameter or power-law exponent. $\Phi(A)$ is the complementary cumulative distribution or survivor function $\Phi(A) = 1 - F(A)$, where F is the cumulative distribution function. For $\beta \leq 1$, the first and second moments are infinite and the associated distribution can be defined as “heavy” (Zaliapin et al. 2005). In general, heavy distributions are typically thought of as wild (e.g., Sornette 2004) in the sense that there are

a large variety of outcomes that can be far from the average. The probability density function for the Pareto distribution is given by

$$f(A) = \beta \frac{A_t^\beta}{A^{\beta+1}} \quad \text{for } A_t \leq A. \quad (2)$$

The tapered Pareto distribution includes a “soft” corner size parameter or turning point A_c applied to the Pareto distribution as an exponential term:

$$\Phi(A) = \left(\frac{A_t}{A}\right)^\beta \exp\left(\frac{A_t - A}{A_c}\right), \quad \text{for } A_t \leq A. \quad (3)$$

The tapered Pareto distribution is an alternative to a truncated Pareto distribution that imposes a “hard” maximum amplitude parameter discussed in the Introduction and shown in Fig. 1. The taper bounds a heavy pure Pareto distribution ($\beta \leq 1$) in the sense that the statistical moments become finite (Kagan and Schoenberg 2001). Vere-Jones et al. (2001) describe the tapered Pareto distribution as being consistent with a maximum entropy distribution in which the mean is fixed and with percolation theory as the correlation length approaches infinity. The pdf of the tapered Pareto distribution is given by

$$f(A) = \left[\frac{\beta}{A} + \frac{1}{A_c}\right] \left(\frac{A_t}{A}\right)^\beta \exp\left(\frac{A_t - A}{A_c}\right) \quad \text{for } A_t \leq A. \quad (4)$$

2.2 Parameter estimation

Several parameter estimation methods have been developed to determine β and A_c for the tapered Pareto distribution. One-parameter estimation methods summarized by Kagan (2002) are those that consider each parameter separately, with the more straightforward estimation of β performed first. To estimate β , the following maximum-likelihood estimate (MLE) is used for the pure Pareto distribution, given n observations (Aki 1965; Kagan 2002):

$$\hat{\beta} = n / \sum_{i=1}^n \ln \frac{A_i}{A_t}. \quad (5)$$

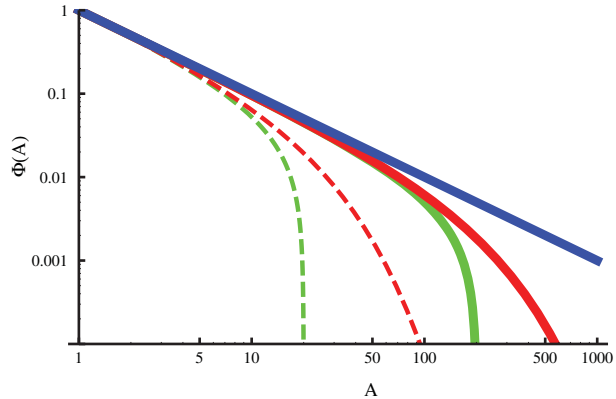
Naylor et al. (2009) indicate that this MLE is equivalent to the results from the generalized linear model (GLM) with Poisson residuals (cf. Charnes et al. 1976). Knopoff and Kagan (1977) indicate that, for data that are power-law-distributed, maximum-likelihood methods are preferred over methods derived from extreme value theory.

For both the tapered or truncated Pareto distributions, the MLE of β is determined by solving the following equation by iteration (Kagan 2002):

$$\frac{1}{\hat{\beta}} - \frac{\ln\left(\frac{A_u}{A_t}\right)}{\left(\frac{A_u}{A_t}\right)^\beta - 1} - \frac{1}{n} \sum_{i=1}^n \ln\left(\frac{A_i}{A_t}\right) = 0, \quad (6)$$

where A_u is an upper limit well above possible values of A_c or the value used to truncate the Pareto distribution. The standard error estimate for β is given by (Deemer and Votaw 1955; Kagan 2002)

Fig. 1 Comparison of Pareto cumulative distribution (blue line) with tapered and truncated Pareto cumulative distribution (red and green lines, respectively: dashed $A_c = 20$; solid $A_c = 200$). For all distributions shown, $\beta = 1$



$$\sigma_{\beta} = \frac{1 - \left(\frac{A_t}{A_u}\right)^{\hat{\beta}}}{\sqrt{n \left\{ \left[1 - \left(\frac{A_t}{A_u}\right)^{\hat{\beta}} \right]^2 \hat{\beta}^{-2} - \left(\frac{A_t}{A_u}\right)^{\hat{\beta}} \left[\ln \left(\frac{A_u}{A_t}\right) \right]^2 \right\}}}. \quad (7)$$

To estimate A_c , Kagan and Schoenberg (2001) developed a method based on the statistical moments of the tapered Pareto distribution, resulting in the following expression:

$$\hat{A}_c = \frac{\frac{1}{n} \sum_{i=1}^n \frac{A_i^2}{n - A_i^2}}{2[A_t \beta + (1 - \beta)A]}. \quad (8)$$

A bias correction factor is indicated by Kagan and Schoenberg (2001), although the root mean square error of the estimate made with the correction factor is larger for small samples than without the correction factor. Other one-parameter methods are described by Kagan and Schoenberg (2001) and Kagan (2002). Expressions to determine standard errors for each parameter are given by Kagan (2002), who indicates that the estimation of A_c is particularly sensitive to the number of samples near A_c . As shown below, in many cases, the likelihood maps are strongly asymmetric along the A_c profile, indicating that a standard error measure of uncertainty is only approximate.

Joint estimation of β and A_c , termed two-parameter estimation, can be made using numerical optimization methods. The log-likelihood function is given by (Kagan 2002)

$$\ell = n\beta \ln A_t + \frac{1}{A_c} \left(nA_t - \sum_{i=1}^n A_i \right) - \beta \sum_{i=1}^n \ln A_i + \sum_{i=1}^n \ln \left(\frac{\beta}{A_i} + \frac{1}{A_c} \right). \quad (9)$$

Vere-Jones et al. (2001) describe an iterative method using Newton–Raphson approximations to determine the two-parameter MLE. In this study, we use the Nelder–Mead direct search method of optimization to find the MLE from Eq. 9 (Nelder and Mead 1965; Press et al. 2007). Because the log-likelihood equation involves the term $1/A_c$, we define $\eta = 1/A_c$ (Kagan and Schoenberg 2001; Kagan 2002) and perform joint MLE on β and η . Meerschaert et al. (2012) further discusses parameter estimation for the tapered Pareto distribution using rank order statistics.

2.3 Likelihood ratios and confidence regions

If we have a set of distribution parameters (θ_0) under a null hypothesis (H_0) where one of the parameters of a more complex distribution in the same distribution family drops out (e.g., as for the pure Pareto distribution compared to the tapered Pareto distribution where A_c drops out), then the likelihood ratio can be used to test whether or not H_0 should be rejected. The test statistic is $2(l - l_0)$, where l and l_0 are the log-likelihood maxima for the tapered Pareto and Pareto distribution, respectively, and is asymptotically distributed as the chi-squared distribution with one degree of freedom $\chi^2_\alpha[1]$ (Kagan 2002). For a particular confidence level α , the test can be written

$$2(\ell - \ell_0) > \chi^2_\alpha[1]. \quad (10)$$

Similarly, confidence regions for the two parameters of the tapered Pareto distribution can be determined using likelihood ratios. The contour (θ_c) for (β, A_c) and (β, η) plots that defines a particular confidence region can be found approximately by equating the likelihood ratio to the chi-squared distribution with two degrees of freedom (i.e., the number of parameters jointly estimated) (e.g., Bird and Kagan 2004):

$$2(\ell - \ell_c) = \chi^2_\alpha[2]. \quad (11)$$

2.4 Sampling

To generate a synthetic sample of length n using a pure Pareto distribution, the following expression is used

$$A = A_t R^{-1/\beta}. \quad (12)$$

where R is a random variable uniformly distributed on the interval (0,1]. For the tapered Pareto distribution, a synthetic sample is generated by selecting the minimum of Eq. 12 and

$$A = A_t - A_c \ln R \quad (13)$$

(Vere-Jones et al. 2001).

For a catalog of finite length, the probability density function of the largest sample in general is given by

$$f_{\max}(A) = nf(A)[F(A)]^{n-1}. \quad (14)$$

The expected value of the largest sample in a catalog for a pure Pareto distribution derived by Newman (2005) is

$$\langle A_{\max} \rangle = nA_t B\left(n, \frac{\beta-1}{\beta}\right) \approx A_t n^{1/\beta}. \quad (15)$$

where B is the beta-function. Thus, the expected largest value of a sampled Pareto distribution depends on the catalog length (n). However, there will be large uncertainty in A_{\max} for any given catalog as expressed by $f_{\max}(A)$. The expression for the expected largest value from a tapered Pareto distribution can be found by numerical computation of Eq. 14 and depends on β and the ratio A_t/A_c .

2.5 Simulations

The range of possible empirical distributions can be determined by drawing multiple catalogs of events with the same sample number from a parent distribution. For example, cumulative distributions of 100 different catalogs are shown in Fig. 2a that are drawn from a pure Pareto distribution using the method described in Sect. 2.4 for $\beta = 1$ and $A_t = 1$. Each catalog contains 50 events. There are significant differences in the apparent tail of the sampled size distribution, with some distributions appearing to be depleted in large events and some distributions appearing to have more abundant large events than the parent Pareto distribution (bold blue lines in Fig. 2a). The “depleted” catalog in this example may be misinterpreted as being distributed according to a tapered Pareto distribution with an artificially low value of A_c (cf. Pisarenko and Sornette 2004) or according to a distribution from a different family with a lighter tail. For the other case shown in Fig. 2a where there are one-to-several large events relative to the parent distribution, the large events may be misinterpreted as “characteristic” or system-wide events that are distinct from the background Pareto distribution (Wesnousky 1994; Kagan 1996). However, several studies have shown that the interpretation of some cases of characteristic events is a consequence of finite sampling (Howell 1985; Stein and Newman 2004; Naylor et al. 2009; Parsons and Geist 2009a; Parsons et al. 2012).

Undersampling may therefore cause us to interpret an observed catalog as having an upper threshold defined by a characteristic event that may not be reflective of the true maximum or most frequent large event. The largest events tend, of course, to have the longest return periods, meaning that nearly every power-law system with a time-limited observation period is subject to undersampling. Thus, before a characteristic interpretation is made, it is important to ensure that this is not a sampling artifact. Naylor et al. (2009) explain that there is both a visual bias for large sizes sampled from a Pareto distribution as well as a sampling bias indicated by a positive skew in the residuals that often lead to a characteristic interpretation.

Shown in Fig. 2b are cumulative distributions for 100 catalogs sampled from a tapered Pareto distribution with the same power-law exponent ($\beta = 1$, $A_t = 1$, $A_c = 20$). As in Fig. 2a, each catalog contains 50 events. In this case, the variation in the tail of the sampled distribution is less than for the pure Pareto distribution, although apparent “depleted” and “characteristic” sampled distributions are still evident as in Fig. 2a.

Increasing the number of events in a catalog decreases the variation in the sampled distribution above a constant minimum probability (Φ_{\min}) as displayed in Fig. 2c, d. Here, Φ_{\min} is determined from the number of samples in the catalogs shown in Fig. 2a, b: $\Phi_{\min} = \frac{1}{50} = 0.02$. Because Figs. 2c and d are plotted at the same scale as Figs. 2a and b, the distribution tail is not shown at lower probabilities. Figures 2e and f display the distributions for $\Phi_{\min} = 0.005$ and 0.001, respectively. Uncertainty in the largest sampled events is similar, because of the self-similarity of the pure Pareto distribution (Naylor et al. 2009). Increasing the number of catalogs displayed (from 100 catalogs in Fig. 2 and 200 catalogs in the examples discussed below) does not significantly affect these results, although outlier distributions are more likely to be present.

The effect of finite sampling on parameter estimation can also be examined. For a pure Pareto distribution with $\beta = 1$, the MLEs of $\hat{\beta}$ are determined for 10^4 catalogs of different lengths ($n = 50, 100, 200$, and 1,000). The mean value and standard error over all catalogs are reported in Table 1. The formula for the standard error $\hat{\beta}/\sqrt{n}$ (Aki 1965; Kagan 2002) is also reported. For this study, standard error estimates are reported in this and other tables

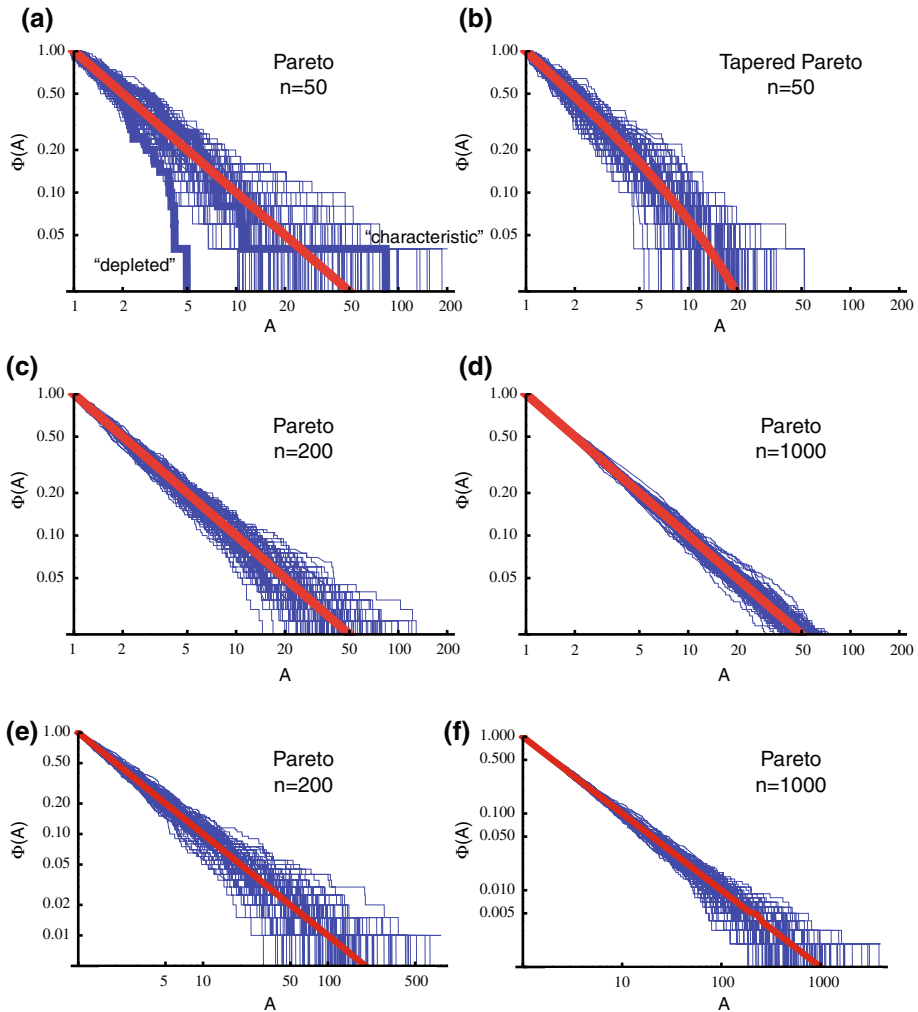


Fig. 2 Examples of 100 cumulative distributions (*blue lines*) sampled from a parent distribution (*red line*). **a** Pareto parent distribution ($\beta = 1$) sampled with catalog length of 50 events. Any single catalog can appear to have depleted or characteristic distribution (*bold blue lines*) relative to the parent distribution. **b** Same as (**a**) except catalogs sampled from a tapered Pareto distribution ($A_c = 20$). **c** Same as (**a**) except catalog length is 200 events. **d** Same as (**a**) except catalog length is 1,000 events. (**e**) and (**f**): Same as (**c**) and (**d**) plotted at the full scale associated with catalog length ($\Phi_{\min} = 0.005$ and 0.001 , respectively)

associated with one-parameter estimation; confidence intervals are indicated in likelihood contour maps for two-parameter estimation results below. Estimates of β improve with larger catalog sizes as indicated in Table 1, although even a catalog size of 50 is able to estimate β of the parent distribution fairly accurately.

For a tapered Pareto distribution, we now examine how sample length affects the parameter estimation of corner amplitude. For $A_c = 20 A_t$ (Table 2), the results of 10^4 catalogs of the same lengths as in Table 1 are shown. As for the pure Pareto distribution, the estimation of β is fairly accurate, although we do not see as large of an improvement in β estimation for larger catalogs. The expression provided by Eq. 7 for the standard error in

Table 1 One-parameter estimation results for 10^4 synthetic catalogs: Pareto distribution $A_t = 1$, $\beta = 1$

n	$\hat{\beta}$	Standard error	$\hat{\beta}/\sqrt{n}$
50	1.022	0.147	0.144
100	1.011	0.102	0.101
200	1.006	0.071	0.071
1,000	1.001	0.032	0.032

β for a tapered Pareto distribution compares favorably with the numerical estimate, as with the pure Pareto distribution. These results indicate that longer catalog lengths are needed to accurately estimate A_c . Refer to Kagan (2002) for additional simulations testing the A_c standard error estimates using the one-parameter techniques.

If A_c is increased to $200 A_t$, there is less chance of having samples near A_c for a given catalog length compared to the previous case where $A_c = 20 A_t$. Results of the one-parameter estimation for this case are shown in Table 3. Because there is proportionally more data to define the power-law component of the distribution for the larger A_c of the parent distribution, there is less error in the β estimate. Conversely, the estimate of A_c is unstable and much less certain than for $A_c = 20 A_t$ (Table 2) and likely meaningless for catalogs less than 1,000 samples.

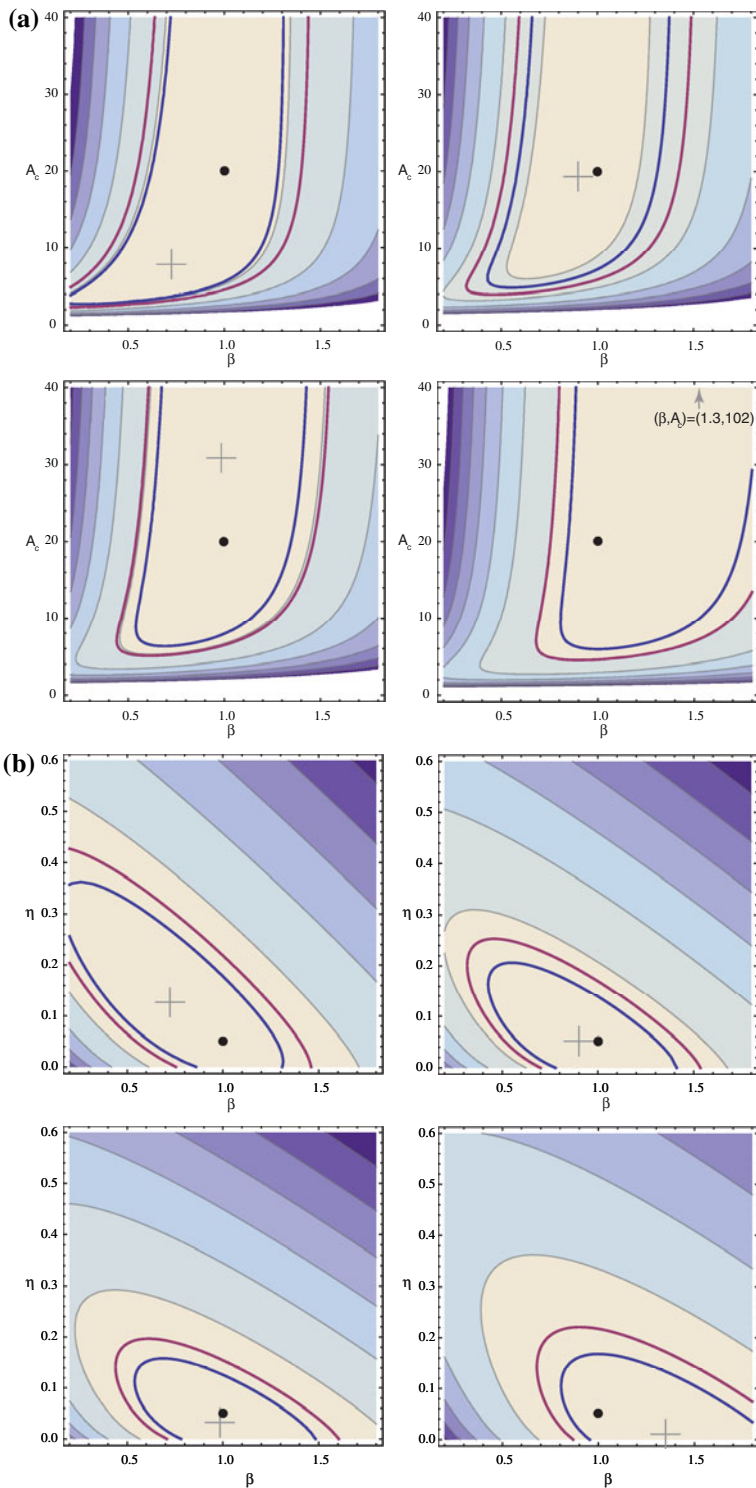
The two-parameter estimation technique jointly estimates β and A_c and yields information of the correlation of likelihood estimates for the two parameters. Shown in Fig. 3a are (β, A_c) likelihood maps for four random catalogs sampled from a tapered Pareto distribution with $A_t = 1$, $A_c = 20$, $\beta = 1$ (dot in each figure) and a catalog length of 50 events in each case. In each case, the MLE is shown by the plus sign and bold lines show the 95 and 99 % confidence contours (see Sect. 2.3). The likelihood maps show strongly asymmetric confidence intervals for A_c , with the lower confidence limit easier to define than the upper confidence limit. As indicated previously, because the likelihood expression in Eq. 9 involves the reciprocal of A_c , we also plot likelihood maps for β and $\eta = 1/A_c$ (Kagan and Schoenberg 2001; Kagan 2002). The (β, η) likelihood maps that correspond to the same four catalogs shown in Fig. 3a are shown in Fig. 3b. In this case, the likelihood contours are ellipsoidal. Thus, the error estimates are more symmetrical than the (β, A_c) maps and can be more easily interpreted in terms of likelihood ratios (Fan et al. 2000). The reciprocal function of A_c in the likelihood function explains the asymmetry in the

Table 2 One-parameter estimation results for 10^4 synthetic catalogs: tapered Pareto distribution $A_t = 1$, $A_c = 20$, $\beta = 1$

n	$\hat{\beta}$	Standard error	Eq. 7	A_c	Standard error
50	1.074	0.186	0.182	21.78	222.7
100	1.063	0.128	0.129	23.12	16.66
200	1.061	0.090	0.091	22.95	10.08
1,000	1.057	0.040	0.040	22.83	4.11

Table 3 One-parameter estimation results for 10^4 synthetic catalogs: tapered Pareto distribution $A_t = 1$, $A_c = 200$, $\beta = 1$

n	$\hat{\beta}$	Standard error	Eq. 7	A_c	Standard error
50	1.028	0.155	0.152	82.6	12,170
100	1.019	0.106	0.106	609.5	24,040
200	1.014	0.075	0.075	178.3	3,655
1,000	1.010	0.033	0.033	210.4	136.0



◀ **Fig. 3** **a** Two-parameter (β , A_c) likelihood contour maps for four random catalogs sampled from a tapered Pareto distribution with $\beta = 1$ and $A_c = 20$ (shown by dot). Catalog length is 50 events. MLE shown by plus sign. 95 and 99 % confidence region shown by blue and magenta lines, respectively. Note that the MLE in the bottom right figure is off the likelihood map. **b** (β , η) likelihood maps for same four catalogs shown in (a), where η is the reciprocal of A_c

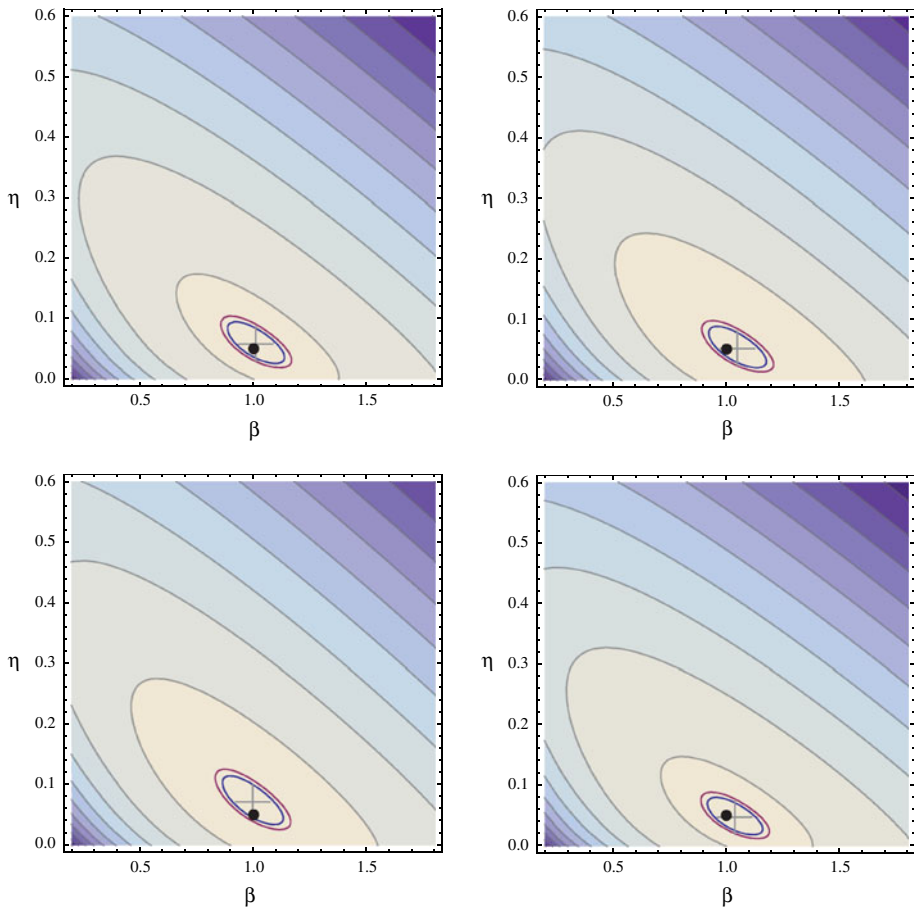


Fig. 4 Same as Fig. 3b with a catalog length of 1,000 events

confidence bounds for A_c and indicates that standard error estimates for A_c may not adequately convey this asymmetry.

In Fig. 3b, the confidence ellipses are sloped indicating a negative correlation in the likelihood estimates for the two parameters: an increase in the estimate for β is compensated by a corresponding decrease in the estimate for η , that is, the estimate of η is affected by the estimate of β —an observation difficult to ascertain from the one-parameter estimation methods described above. Moreover, for cases where the estimates of the two parameters are dependent (i.e., inclined axes of contour ellipsoids), the likelihood ratio test

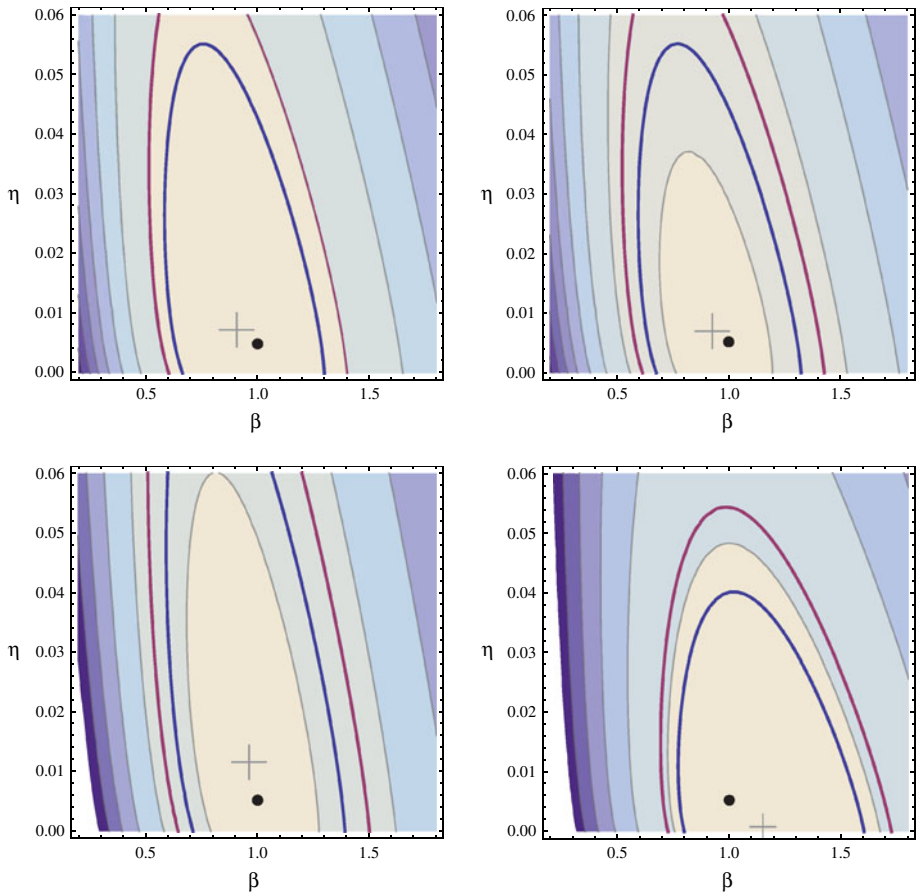


Fig. 5 Same as Fig. 3 sampled from a tapered Pareto distribution with $\beta = 1$ and $A_c = 200$ (shown by dot). Catalog length is 50 events

based on a profile at the MLE for β may not yield a comprehensive result. As shown in the case of Fig. 3b (top left), the likelihood ratio taken along a profile of $\hat{\beta}$ would falsify the null hypothesis ($\eta = 0$; $A_c \rightarrow \infty$) at the 95 % confidence level. However, there exists other estimates of β within the 95 % confidence region in which the null hypothesis is true. In all four cases shown in Fig. 3b, there is a range of β estimates for a pure Pareto distribution ($\eta = 0$) within the 95 and 99 % confidence, even though the synthetic catalog was sampled from a tapered Pareto distribution. Thus, for small catalog lengths, we may not be able to tell whether a given catalog follows a pure Pareto distribution or not.

Figure 4 shows the two-parameter estimates for a catalog length of 1,000, using the same parent distribution as in Fig. 3. As expected, the uncertainty in estimating both parameters greatly decreases with the longer catalog. The axes in the confidence ellipses are still inclined, indicating dependency in estimates of the two parameters. However, the confidence ellipses do not intersect $\eta = 0$ indicating that the pure Pareto null hypothesis can be falsified for the longer catalog.

In Figs. 5 and 6, the catalogs are sampled from a tapered Pareto distribution with $\beta = 1$ and $A_c = 200$ (A_t remains fixed at 1). The uncertainty in β significantly decreases with the

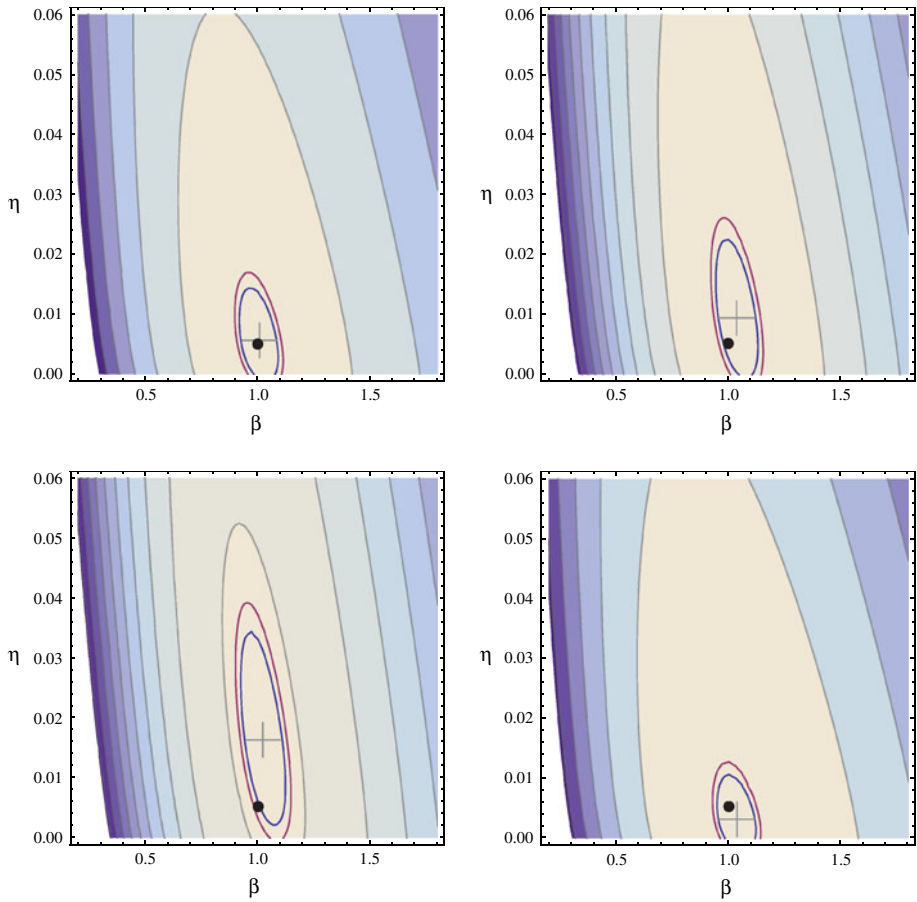


Fig. 6 Same as Fig. 5 with a catalog length of 1,000 events

1,000-event catalog (Fig. 6) compared to the 50-event catalog (Fig. 5). However, in this case, where the ratio of A_c to A_t is large, significant uncertainty remains in η and the confidence contours frequently intersect the $\eta = 0$ axis. Thus, the upper confidence bound of A_c , even for the 1,000-event catalog, is difficult to ascertain for large differences between A_c and A_t . In both cases, the confidence contours are more aligned with the axes than for a parent distribution with $A_c = 20$ (Figs. 3, 4), suggesting that the likelihood estimation for the two parameters is roughly independent.

3 Examples of undersampling effects for observed natural hazards

Three examples demonstrating the effect that undersampling hazards governed by Pareto-type distributions are described in this section. The first two examples relate to hazards as they impact particular sites: tide gauge stations in the case of tsunamis (Sect. 3.1) and hydrologic stations in the case of floods (Sect. 3.2). The third example deals with a hazard source, subduction earthquakes measured by seismic moment, rather than the hazard itself

(i.e., ground motion). The tsunami and flood hazard examples aggregate different types of sources (e.g., tsunamigenic sources and precipitation events) and include the effects of propagation from the source to the site. Because these effects are site- and region-specific, global analysis of these hazards would result in mixed distributions and is not performed. The earthquake example is included to determine the effects of undersampling on globally distributed hazard sources, though mixed distributions may still be an issue as discussed in Sect. 3.3.

3.1 Tsunamis

An analysis of the historical record of tsunamis is often the basis for siting and designing critical facilities, such as nuclear power plants near the coast and tsunami defense structures (e.g., JSCE 2002; Sato et al. 2003; Yanagisawa et al. 2007; Prasad 2009; Shuto and Fujima 2009). Typically, some measure of uncertainty related to the limitations of the historical record is accounted for in these hazard assessments, although the possible tsunami sources and outcomes are strongly constrained by historical precedent. Part of the reason for using the historical record as a starting point for tsunami hazard assessment relates to viewing tsunamis within a hydrologic spectrum of floods: specifically, as part of estimating the “probable maximum flood” from a variety of phenomena (storm surge, riverine flooding, tsunamis, etc.) (Yen 1988; IAEA 2011). For this reason, we examine how well the historical record defines the distribution of tsunami sizes, with particular attention to quantifying the uncertainty in estimating the size and probability of extreme events.

Determining empirical size distributions for tsunamis has been discussed in several previous studies (Soloviev 1970; Nakamura 1979; Horikawa and Shuto 1983; Kulikov et al. 2005). The study by Burroughs and Tebbens (2005) was one of the first to recognize that tsunami data at small amplitudes tend to fit a power-law distribution. Toward large amplitudes, the power-law distribution is assumed to be truncated in the discrete form, although it has been unclear whether upper truncation that best fits the data is related to sampling limitations or in the physics controlling tsunami size (Burroughs and Tebbens 2001). Moreover, there has not been an analysis of parametric uncertainty associated with empirical tsunami size distributions. We use the methods described in Sect. 2 and the long record of frequent tsunamis in Japan to determine the effect that a single extreme event (i.e., the 2011 Tohoku-oki tsunami) has on the empirical tsunami size distribution.

3.1.1 Data selection

Although there are a variety of available tsunami measurements, tide gauge records provide as close to a homogeneous tsunami catalog as possible. For the purpose of this study, a tide gauge station-specific catalog of events is selected in which the maximum tsunami amplitude for a given event is compiled (http://www.ngdc.noaa.gov/hazard/tsu_db.shtml). Inclusion of other tsunami data, such as eyewitness observations, post-tsunami surveys, and paleotsunami deposits, would increase the size and duration of the tsunami catalog, but would also result in a mixed catalog that spans a finite geographic area rather than being specific to a single location. Measurement uncertainty, censoring, and mixed measurement types would be considerable obstacles in a statistical analysis of such a catalog (Geist and Parsons 2006; Geist et al. 2009).

Although there are many tide gauge stations and offshore observatories that measured the size of the 2011 Tohoku-oki tsunami, we focus on the data from the Miyako tide gauge station in Japan. This station has a long history of recording tsunamis and is a station that is

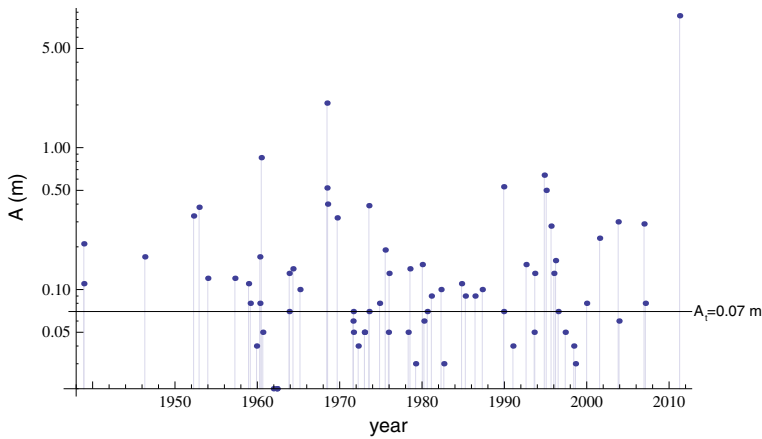


Fig. 7 Catalog of maximum tsunami amplitude per event (A) for the Miyako tide gauge station. Amplitude given on a logarithmic scale

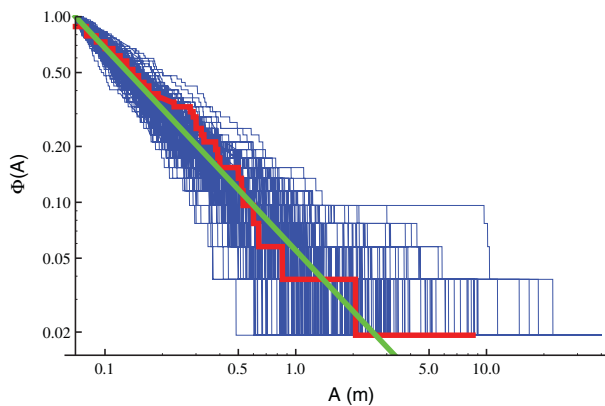


Fig. 8 Empirical cumulative distribution of the data shown in Fig. 7 (red line) in comparison with 200 synthetic catalogs (blue lines) sampled from a pure Pareto distribution (green line) with β estimated from the one-parameter method ($\beta = 1.01$)

Table 4 Parameter estimates of Pareto and tapered Pareto distributions

	Pareto	Tapered Pareto	
	$\hat{\beta} \pm \sigma_{\beta}$	$\hat{\beta} \pm \sigma_{\beta}$	$\hat{A}_c \pm \sigma_{A_c}$ (m)
Without Tohoku-oki	1.09 ± 0.15	1.09 ± 0.21	1.36 ± 1.16
With Tohoku-oki	1.01 ± 0.14	0.99 ± 0.15	11.2 ± 22.7

close to the earthquake source of the 2011 tsunami. The maximum amplitude of the 2011 Tohoku-oki tsunami recorded at the Miyako station is reported to be 8.5 m. The size of the tsunami, however, may have been greater than this because the tide gauge station was disrupted by the tsunami (Ozaki 2011). The nearby off-Miyako GPS buoy recorded more

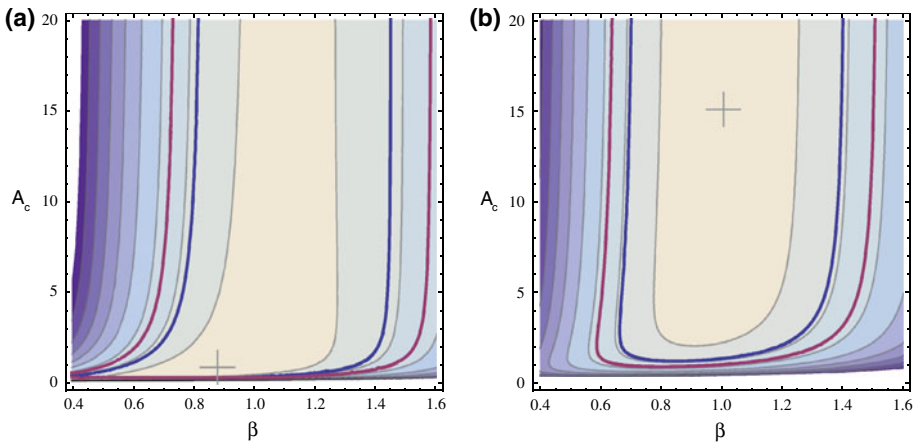


Fig. 9 Two-parameter (β , A_c) likelihood contour maps for the Miyako tide gauge catalog **a** without and **b** with the 2011 events. Catalog lengths are 51 and 52 events, respectively. MLE shown by plus sign. 95 and 99 % confidence interval in parameter estimates shown by blue and magenta lines, respectively

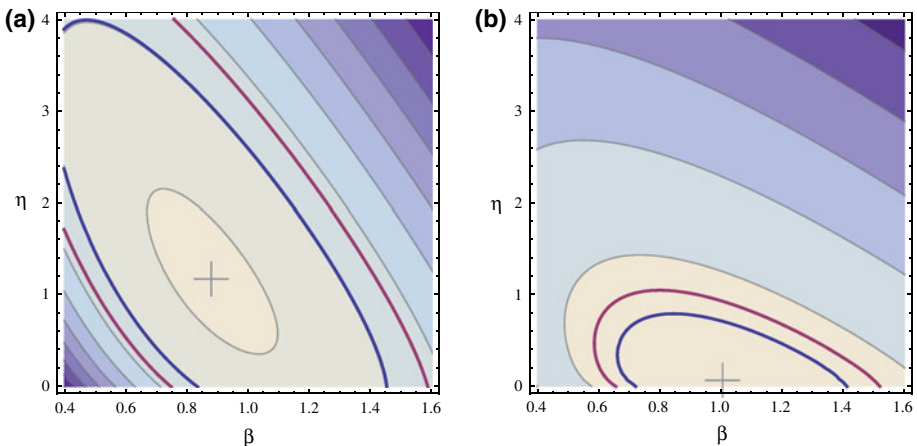


Fig. 10 Two-parameter (β , η) likelihood contour maps for the same data as analyzed in Fig. 9

of the waveform than the tide gauge station (Ozaki 2011), suggesting that the Miyako tide gauge station recorded the largest amplitude of the direct wave. We will use 8.5 m as the maximum for the 2011 event at the Miyako station for the analysis presented below.

3.1.2 Results

Data from the Miyako tide gauge station is evaluated with respect to the Pareto and tapered Pareto distributions (Fig. 7). For the data considered in this study, $A_t = 0.07$ m as determined by evaluating censoring effects and the recording threshold for tsunamis in the

presence of ambient noise from wind waves (cf. Rabinovich and Stephenson 2004; Geist and Parsons 2011). The empirical cumulative distribution of the data is shown in Fig. 8 (red line) in comparison with the cumulative distribution of 200 synthetic catalogs (blue lines) with the same catalog length ($n = 52$) sampled from a pure Pareto distribution with $\beta = 1.01$ (green line; see below for parameter estimation results). The synthetic catalogs form a trumpet-shaped envelope of distributions (cf. Main et al. 2011). The data both with and without the 2011 event are within the envelope defined by the synthetic catalogs. The empirical cumulative distribution of the catalog with the 2011 event appears to contain a characteristic event, but this is an artifact of sampling the Pareto distribution as described in Sect. 2.

The distribution parameters for the Miyako tide gauge station are estimated both with and without the 2011 Tohoku-oki tsunami. The parameters and error estimates for both the Pareto and tapered Pareto distributions using the one-parameter methods described in Sect. 2 are listed in Table 4. There are only small changes in β with the inclusion of the 2011 Tohoku-oki event. In contrast, the change in the estimated A_c value is considerable. Moreover, the log-likelihood curve is flatter resulting in a very large error estimate in A_c when the 2011 event is included. Conventional asymptotic expressions for standard error may be heavily biased for the sample size considered here.

Results of the joint two-parameter estimation method are shown in Figs. 9 and 10. The (β, A_c) likelihood maps indicate a large discrepancy between the estimates of A_c with and without the 2011 Japan tsunami measurement, similar to the one-parameter results. Without the 2011 event, A_c is estimated to be 0.85 m, whereas with the 2011, A_c is estimated to be 15.1 m (cf. with the one-parameter results Table 4). It should be noted that the 15.1 m estimate is within the wide confidence regions displayed in Fig. 9a. The estimates of β are 0.88 and 0.91, without and with the 2011 events, respectively, slightly lower than estimates using the one-parameter method (Table 4). Shown in Fig. 10 are the (β, η) likelihood maps. These maps indicate that the pure Pareto distribution cannot be rejected for either of these catalogs (with or without the 2011 event) at the 95 or 99 % confidence level.

3.2 Floods

Traditionally, several different families of probability distributions have been used to describe stream flows. These include distributions from the normal family (normal, log-normal, and 3-parameter lognormal), generalized extreme value distribution, and the Pearson type III family of distributions (Stedinger et al. 1993). It is worth noting that power-law-type distributions have been suggested for flooding as conservative alternatives to conventional size distributions such as the log Pearson type III distribution (Kidson and Richards 2005; Malamud and Turcotte 2006). Turcotte and Haselton (1996) showed that historical records from US Geological Survey (USGS) hydrologic stations are well fit by a Pareto distribution, with the power-law exponent varying according to climate. Malamud et al. (1996) model Mississippi River flooding records with a power-law relationship, who, along with Kidson and Richards (2005), indicate that the power-law models yield more conservative estimates for extreme flooding events. These estimates are also consistent with paleoflood data (Malamud et al. 1996; Malamud and Turcotte 2006). We examine the data from to US hydrologic stations in different climate regions that were modeled using a power-law relation by Turcotte and Green (1993) and Malamud and Turcotte (2006) to determine whether or not a corner size parameter for stream flow can be confidently estimated.

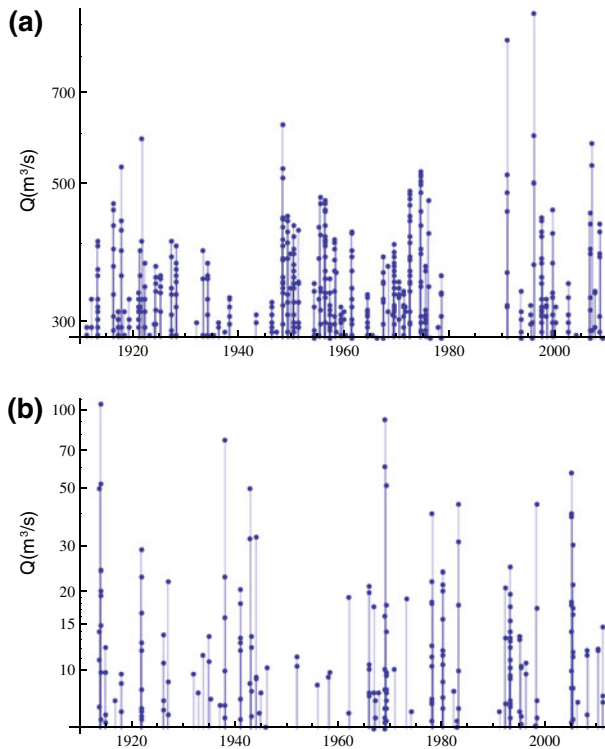


Fig. 11 Catalog of daily mean stream flow greater than A_t for **a** Wenatchee River, Washington, and **b** Arroyo Seco, California, stations. Stream flow given on a logarithmic scale

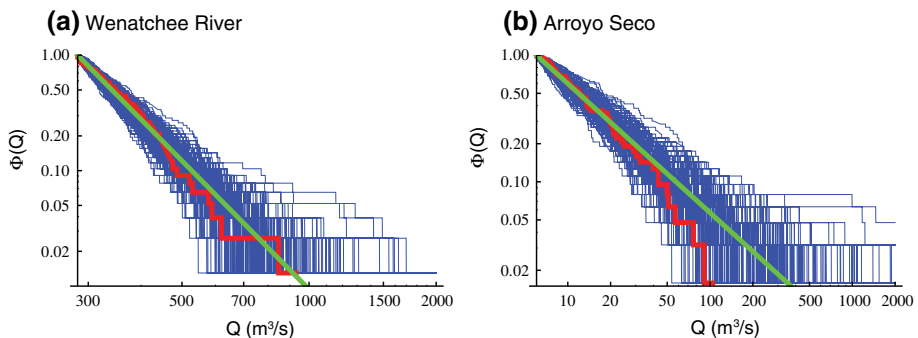


Fig. 12 Empirical cumulative distribution of the data shown in Fig. 11 (red line) in comparison to 200 synthetic catalogs (blue lines) sampled from a pure Pareto distribution (green line) with β estimated from the one-parameter method ($\beta = 3.74, 1.10$, respectively)

3.2.1 Data selection

Partial duration flood series are derived from USGS hydrologic station data. The procedure to determine the partial duration floods from daily discharge data is described by Malamud and Turcotte (2006). As explained by these authors, partial duration flood series is

Table 5 Parameter estimates of Pareto and tapered Pareto distributions

	Pareto	Tapered Pareto	
	$\hat{\beta} \pm \sigma_{\beta}$	$\hat{\beta} \pm \sigma_{\beta}$	$\hat{Q}_c \pm \sigma_{Q_c} \text{ (m}^3\text{/s)}$
Wenatchee River	3.74 ± 0.43	3.72 ± 0.43	$2,390 \pm 1,500$
Arroyo Seco	1.10 ± 0.14	1.02 ± 0.21	67.4 ± 36.2

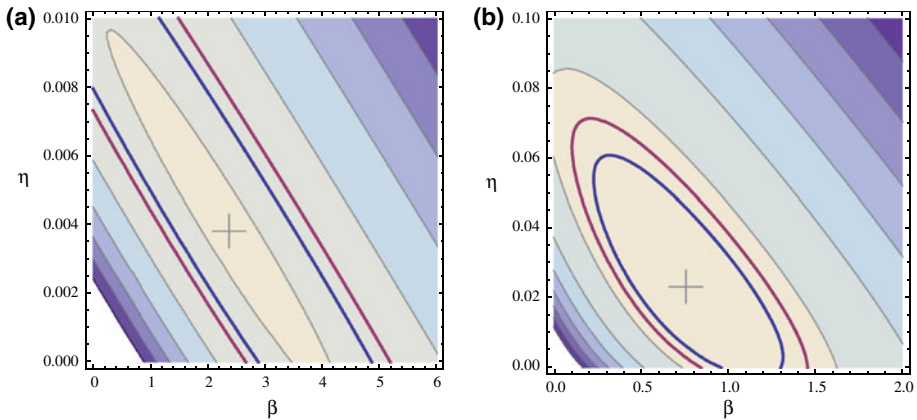


Fig. 13 Two-parameter (β , η) likelihood contour maps for **a** the Wenatchee River and **b** Arroyo Seco catalogs. Catalog lengths are 77 and 63 events, respectively. MLE shown by plus sign. 95 and 99 % confidence interval in parameter estimates shown by *blue* and *magenta* lines, respectively

preferred over annual flood series because there may be several major floods in a given year and these floods may be larger than an annual flood in another year. Thus, annual flood series may be statistically biased in terms of the number and size of floods recorded at a station. In an attempt to determine statistically independent floods, maximum daily mean stream flows are separated by a specified number of days: in this study, as in Malamud and Turcotte (2006), 30 days are used. The number of partial duration floods for a particular station catalog is limited to the number of water years encompassed by the catalog. Malamud and Turcotte (2006) provide further details of the procedure used.

Two station catalogs in different climate regions are analyzed and compared: Arroyo Seco near Pasadena, California; Wenatchee River in the state of Washington (Fig. 11). The Arroyo Seco station is in a semiarid region with a small drainage area (41 km²). The peak daily mean stream flow within the catalog that spans the years 1914–2010 is 104 m³/s, occurring on February 20, 1914. The Wenatchee River station is in a maritime climate region with a much larger drainage area of 1,531 km². The peak daily mean stream flow within the catalog that spans the years 1911–2008 is 932 m³/s, occurring on November 30, 1995.

The empirical cumulative distributions for the two catalogs are shown in Fig. 12 (red lines). The Wenatchee River distribution follows closely to the pure Pareto distribution (green line). In contrast, the Arroyo Seco distribution falls off at high stream flow values. Although the empirical distribution shown in Fig. 12b is within the envelope of 200 synthetic distributions, it is on the depleted side of the envelope. We discuss whether a corner stream flow can be estimated for this station in the analysis below.

3.2.2 Results

The parameters for the Pareto and tapered Pareto distributions using the one-parameter methods are listed in Table 5. There are significant differences in $\hat{\beta}$ between the two stations, with the Arroyo Seco station having a heavier tail. The value of β appears to be influenced primarily by climate (Turcotte and Green 1993; Turcotte and Haselton 1996). The estimated corner stream flow parameter \hat{Q}_c for the Wenatchee River station is significantly higher than the maximum mean-daily stream flow in the catalog, indicating that this estimate is suspect. (The expected value of A_{\max} is 1,072 m³/s from Eq. 15.) In contract, \hat{Q}_c for the Arroyo Seco station is well within the range of the catalog. In both cases, the standard error estimate is large relative to the estimated value.

Results of the joint two-parameter estimation (β , η) for the Wenatchee River and Arroyo Seco stations are shown in Fig. 13. The estimates of β are 2.37 and 0.77, respectively, lower than the estimates from the one-parameter methods. Inclination of the maximum-likelihood contours indicates dependence between the estimates of β and η . The 95 and 99 % confidence regions for the Wenatchee River station (Fig. 13a) intersect the $\eta = 0$ axis, indicating that the pure Pareto distribution cannot be rejected. We are almost able to reject the pure Pareto distribution for the Arroyo Seco station: the confidence regions barely intersect the $\eta = 0$ axis, consistent with the results shown in Fig. 12b.

3.3 Subduction zone earthquakes

It is well known that earthquakes in general follow a power-law distribution of sizes (Ishimoto and Iida 1939), often referred to as the Gutenberg–Richter relation (Gutenberg and Richter 1944). Various forms of a modified Pareto distribution have been used to model global catalogs of seismic moment (M). The moment magnitude (m_w) of an earthquake is defined as a logarithmic function of seismic moment (Hanks and Kanamori 1979):

$$m_w = \frac{2}{3}(\log_{10} M - 9.05) \quad (16)$$

Various zonation schemes have been used for earthquakes, including the Flinn–Engdahl regions based on geographic boundaries (Flinn et al. 1974). For this study, we use earthquake zones based on plate tectonic boundary type, focusing on earthquakes within a

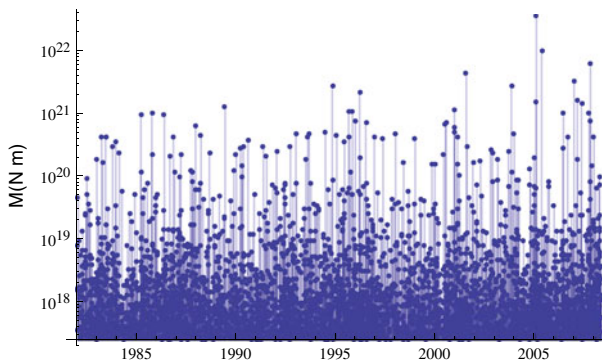


Fig. 14 Catalog of global subduction zone earthquakes as specified by Kagan et al. (2010). Seismic moment given on a logarithmic scale

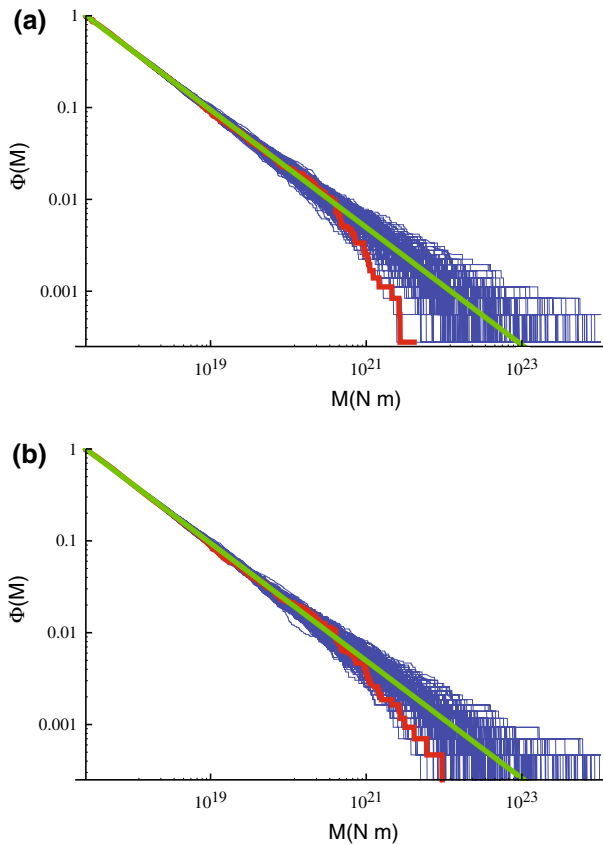


Fig. 15 Empirical cumulative distribution of the data shown in Fig. 14 (red line) in comparison with 200 synthetic catalogs (blue lines) sampled from a pure Pareto distribution (green line) with β estimated from the two-parameter method ($\beta = 0.64$). **a** Global CMT catalog of subduction zone earthquakes January 1, 1982–December 25, 2004. **b** Global CMT catalog of subduction zone earthquakes January 1, 1982–March 31, 2008

maximum horizontal distance from a subduction zone plate boundary as specified by Bird and Kagan (2004). Bird and Kagan (2004) found that tectonic boundaries and intraplate regions can have distinctive distribution parameters, particularly with regard to the corner magnitude. The global Centroid Moment Tensor (CMT) earthquake catalog is used to analyze the distribution of seismic moment near subduction zones, where most of the largest earthquakes occur. By coincidence, the first three-fourths of the catalog that started in 1977 with the advent of broadband seismometry contain no $m \geq 9$ earthquakes—prior to the December 26, 2004 Sumatra–Andaman earthquake, the last $m \geq 9$ earthquake was in 1964. We examine the effects of a lack of large earthquakes on parameter estimation by separately analyzing the global CMT catalog of earthquakes up to December 26, 2004 and the entire global CMT.

3.3.1 Data selection

Earthquakes within the “trench zone” as defined by Kagan et al. (2010) were used for this analysis. The catalog includes earthquakes from January 1, 1982 through March 31, 2008,

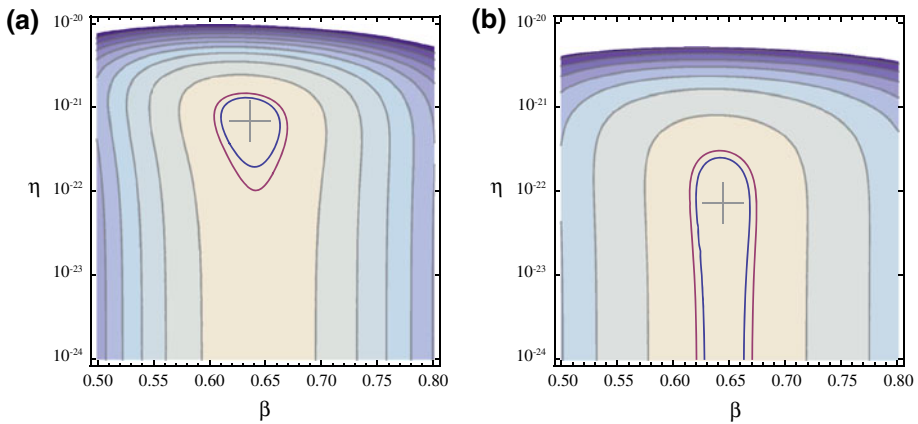


Fig. 16 Two-parameter (β , η) likelihood contour maps (logarithmic η axis) for **a** 1982–2004 and **b** 1982–2008 catalogs. Catalog lengths are 3,586 and 4,283 events, respectively. MLE shown by plus sign. 95 and 99 % confidence interval in parameter estimates shown by blue and magenta lines, respectively

which is complete at a threshold m_w of 5.6 (Bird et al. 2002), and at depths shallower than 70 km. The trench zone includes earthquakes that occur within 186 km of oceanic convergence plate boundaries and within 220 km landward and 135 km seaward of subduction zone plate boundaries as indicated in Bird and Kagan (2004). The locations of the plate boundaries are defined in Bird (2003). Earthquakes in the trench zone also include intra-plate earthquakes in the outer rise and within the overriding plate. A total of 4,283 earthquakes are analyzed (Fig. 14).

Two empirical cumulative distributions are shown in Fig. 15: one for the sub-catalog up to, but not including, the December 26, 2004 $m_w = 9.0$ Sumatra–Andaman earthquake (Fig. 15a) and one for the entire catalog (Fig. 15b). Eight earthquakes with $m_w > 8$ have occurred since the 2004 Sumatra–Andaman event. As with the other natural hazards examined, the empirical distributions are compared with 200 synthetic catalogs of the same length sampled from a pure Pareto distribution with the MLE of β . The sub-catalog up to December 26, 2004 (Fig. 15a) appears depleted, falling to the left of the 200 synthetic distributions sampled from a pure Pareto distribution. The distribution of the entire catalog (Fig. 15b), including the recent large-magnitude earthquakes, falls within the envelope of synthetic catalog distributions. (The width of this envelope will slightly depend on the number of synthetic distributions used.)

3.3.2 Results

Results of the joint two-parameter estimation (β , η) for the two catalogs are shown in Fig. 16. In contrast to the other natural hazards presented, the axis for η is given on a logarithmic scale for presentation purposes. The estimate of β is 0.64 for both catalogs and is well constrained, although Kagan (2010) describes several factors that cause an upward bias in the estimate of β for earthquakes. The estimates of M_c are 8.11 for the 1982–2004 catalog and 8.76 for the 1982–2008 catalog. The latter results replicate results obtained by Kagan et al. (2010). There appears to be little inclination of the likelihood contours, suggesting independence between the estimates of β and η , relative to the other natural hazards examined (see Kagan 2002 for further discussion).

The interesting result of this analysis is that 95 and 99 % confidence regions shown in Fig. 16a (and even the 99.9 % confidence region not shown) for the 1982–2004 catalog are closed, suggesting that a pure Pareto parent distribution can be rejected with confidence. However, when more recent earthquakes are included, the contours intersect the $\eta = 0$ axis (not shown because of the logarithmic scaling), indicating that the pure Pareto distribution cannot be rejected. Similar conclusions were reached by Zöller (2013) in a statistical analysis of the entire global CMT catalog. In addition, the MLE of η using the full catalog (1982–2008) is outside of the 99 % confidence region defined by the 1982–2004 sub-catalog.

Main et al. (2008) show that adding shallow earthquakes in the global CMT catalog through December 2006, including the 2004 Sumatra–Andaman, effectively shifts the moment distribution to a pure Pareto from a tapered Pareto distribution determined for the 1977–1999 catalog. In addition, Bird and Kagan (2004) calculate a much higher $m_c = 9.58$ for the pre-2004 global CMT catalog merged with the Pacheco and Sykes (1992) catalog starting in 1900 and using tectonic constraints on seismic moment release rate (see also Kagan and Jackson 2013). Thus, forecasting the maximum magnitude of global subduction earthquakes is strongly dependent on the nature of the input catalog, and one can be badly misled (at high confidence) if the input data are not fully understood.

This issue naturally leads back to the definition of confidence region or interval. A confidence interval is a random interval dependent on the particular sample used for calculating the interval (Rice 2007). Typically, the definition is that if an experiment is repeated many times, the confidence region would include the true value of a parameter 95, 99 %, etc., of the time. The historical record of natural hazards is non-repeatable, but confidence is conferred by statistical power from a large sample size, and the input distribution's resemblance to the one being tested. While it is reasonable to search for a corner parameter that defines the size distribution of subduction zone earthquakes (i.e., $\eta > 0$) by examining a large catalog of them as we have done, it is worth noting some pitfalls.

One important pitfall is excessive aggregation of observations, which might apply to any empirically based forecast. In the present example, the effort to secure a large global catalog of subduction earthquakes could result in a stacked group of mixed distributions, each representing independent undersampled processes. Indeed, individual global subduction zone convergence rates, geometries, and geologic settings vary strongly (e.g., Stern 2002). McCaffrey (2008) divided global subduction zones into 32 regions with independent mean recurrence times for the largest moment events ranging from 191–1734 years. Under this concept, it would be very possible that the tested 1982–2004 period would not have observed sufficient numbers of high-magnitude events to properly characterize a tapered Pareto distribution. In other words, the apparently robust 3,586 event catalog is really an aggregate of ~ 32 independent catalogs consisting of ~ 100 events each.

We model this effect using a simple earthquake simulator that was tested for the Nankai subduction zone in Japan, the San Andreas fault in California, and the Wasatch fault in Utah (Parsons and Geist 2009a; Parsons et al. 2012). We must use synthetic catalogs for this test because that is the only way to assess the completeness of high-magnitude events, because the parent magnitude frequency distributions are known and pre-defined. The method assigns earthquakes of initial magnitude randomly sampled from a Gutenberg–Richter relation (pure Pareto distribution), but modifies them according to slip rate, fault geometry, and strain budget based on prior events. Systems are thus allowed to develop characteristic magnitudes if needed to fit observations. We use this technique to develop individual synthetic earthquake catalogs for 32 subduction zones as defined by McCaffrey (2008) scaled for the 1982–2004 time interval and then perform the same MLE analysis as was done for the real catalog in Fig. 16a.

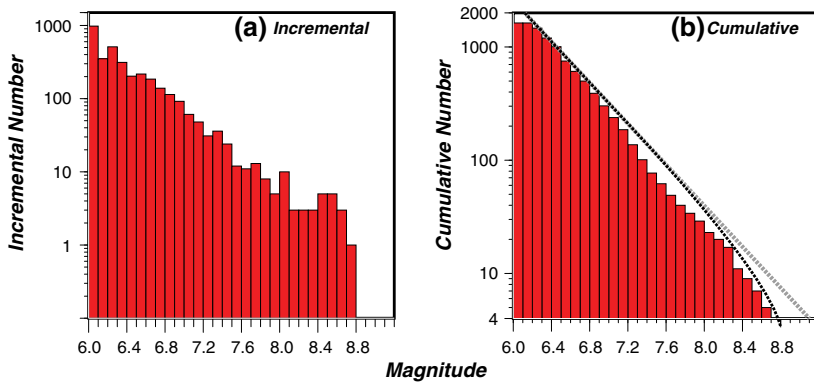
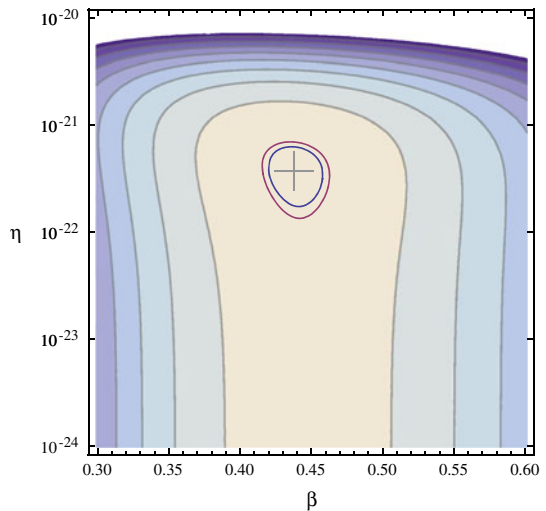


Fig. 17 **a** Incremental and **b** cumulative magnitude frequency distributions from 32 synthetic subduction zone catalogs generated from a simple earthquake simulator. The stacked catalogs each report different maximum observed magnitudes, which creates the appearance of a tapered Pareto distribution (*black dashed line*), whereas each catalog is actually undersampled

Fig. 18 Two-parameter (β , η) likelihood contour maps (logarithmic η axis) for synthetic subduction zone catalog generated from a simple earthquake simulator. MLE shown by plus sign. 95 and 99 % confidence interval in parameter estimates shown by *blue* and *magenta* lines, respectively



The results of our modeling exercise are quite similar to the real catalog, with a modeled corner magnitude of $m_c = 8.3$ as compared with $m_c = 8.1$ from the real catalog. The individual catalogs each have a maximum reported magnitude that creates an apparent Pareto taper such that the confidence intervals on the corner moment are overfit to high confidence (Figs. 17, 18).

The occurrence of several $m \geq 8.6$ earthquakes since 2004 is inconsistent with the 1982–2004 corner moment analysis despite its apparent high degree of significance. The result shown in Fig. 16b suggests that a corner moment greater than equal 10^{24} ($m_c \geq 9.94$) or any other arbitrary high value cannot be excluded at the 99 % confidence level. These results do lend caution to interpreting a likelihood-based upper bound to a corner size from a catalog depleted in large events. We suggest that increasing sample size by aggregating multiple undersampled catalogs can produce a distribution that, while fit to a high degree of confidence, may not adequately represent the full hazard.

4 Discussion

Throughout this study, we have compared the unbounded pure Pareto distribution to the tapered Pareto distribution using natural hazards catalog data. Parameter estimation of both distributions was performed, with the tapered Pareto distribution specified by a corner size parameter A_c that dictates the location of the exponential taper, in addition to the power-law scaling exponent β . In most cases, likelihood-based methods can specify β for both distributions with reasonable accuracy and approximately symmetric upper and lower bounds. In contrast, estimates of A_c are unstable and the confidence bounds are strongly asymmetric, with the upper confidence bound typically not determined. (The confidence bounds are symmetric, rather, in terms of $\eta = 1/A_c$). Using likelihood ratios, the pure Pareto null hypothesis could not be rejected for each natural hazard example examined except the 1982–2004 sub-catalog of subduction zone earthquakes, though, as discussed above, the tapered Pareto fit to the subduction catalog is likely a result of mixing multiple distributions. The occurrence of several $m \geq 8.6$ earthquakes since 2004 supports a pure Pareto model.

Although a pure Pareto distribution is the simplest model supported by a statistical analysis of the data, this model presents considerable difficulties in hazard assessments that require specification of a deterministic “maximum” severity or cumulative economic loss, owing to the fact that such a distribution is scale free. There are certainly physical controls on natural hazard size. For example, tsunami size is limited by turbulent attenuation from wave breaking and bottom boundary-layer flow near shore (Lynett et al. 2002; Korycansky and Lynett 2005); conceptually, earthquake size is limited by the available fault rupture dimensions and slip (e.g., Wyss 1979). This study demonstrates that while there are physical mechanisms that limit the size of the natural hazard, in most cases, we cannot confidently determine the deviation from Pareto of the size distribution tail using historical data.

Because of the difficulty in estimating a maximum size from historical data, deterministic assessments that estimate the maximum severity of a hazard are prone to significant uncertainty that typically is not conveyed in these assessments. However, in many applications, the hazard can be defined probabilistically. For example, a deterministic “probable maximum tsunami” used to assess the tsunami risk at US nuclear power plants (Yen 1988; Prasad 2009; IAEA 2011) could be replaced with a design probability specification for use in a performance-based risk analysis (Porter et al. 2007). Zaliapin et al. (2005) also develop methods to calculate sums from a pure Pareto in estimating cumulative economic losses. Marzocchi et al. (2012) review Bayesian methods to apply pre-calculated and operational hazard probability to better inform evacuation decisions compared to deterministic tools.

Probabilistic hazard assessments can incorporate limiting conditions on hazard size by incorporating physical constraints to the size of the hazard source (e.g., moment conservation for earthquakes) and by determining the effects of propagation between source and site (e.g., seismic attenuation relations for earthquakes and unit hydrographs for floods). For example, probabilistic tsunami hazard analysis (PTHA) (Geist and Parsons 2006; Parsons and Geist 2009b) can compute the tsunami size distribution at a site through the use of numerical propagation and runup models that include the effects of shoaling amplification, dispersion, refractive focusing, scattering, wave trapping, and wave breaking. However, the resulting hazard curve (that includes an estimate of activity rate and an assumed inter-event time distribution) is critically dependent on the earthquake moment distribution input to PTHA. For example, if historical earthquakes are used as the basis for

developing tsunami hazard curves (e.g., Rikitake and Aida 1988; Annaka et al. 2007), PTHA can underestimate the hazard in a similar manner as for the empirical analysis of the hazard explained in this paper. Rather, for coastlines along subduction margins, it is likely that earthquake sizes follow a modified Pareto distribution with a higher corner magnitude determined from both a moment conservation principal and catalog data ($m_w > 9.1$) than indicated solely from regional historical data (Bird and Kagan 2004). Theoretical limits to source or hazard size themselves may be subject to considerable epistemic uncertainty that can be incorporated in a logic tree framework (e.g., Field et al. 2009). Finally, empirical analyses can be combined with computational PTHA to yield a better representation of uncertainty in tsunami hazard estimation (Parsons and Geist 2009b; Grezio et al. 2010).

5 Conclusions

In examining the effects of undersampling of natural hazards that exhibit power-law scaling, several key findings have been made as described below:

1. The tails of empirical distributions generated from synthetic catalogs sampled from a pure Pareto distribution deviate from the parent distribution and take on a trumpet-shaped envelope (Naylor et al. 2009; Main et al. 2011) with two general effects (Fig. 2):
 - a. In some cases, the tail of an empirical distribution is dominated by one-to-several large events, sometimes interpreted as system-wide, or characteristic events. For example, a characteristic earthquake fully ruptures a fault segment and a “characteristic” tsunami is the tsunami that is generated from such an event. However, this is also consistent with artifacts of finite sampling of a Pareto distribution.
 - b. In other cases, the tail of an empirical distribution appears depleted relative to a pure Pareto distribution. This too can be an artifact of finite sampling and the distribution can change dramatically with the addition of even one large event. The apparent depleted empirical distribution is more difficult to diagnose than the apparent characteristic events, in that the former appears as an exponentially tapered Pareto distribution with a low corner size.
2. Whereas the corner size (A_c) of a given natural hazard can be estimated from many catalogs, the upper confidence bound cannot be determined, such that the pure Pareto distribution cannot be rejected from a statistical standpoint.
3. In cases where the measurement threshold for a natural hazard is within several orders of magnitude of a corner size (if it exists), the estimates of corner size and the power-law scaling exponent are dependent on one another. Joint, two-parameter estimation techniques are often required. In addition, traditional profile-based likelihood ratio tests may not detect cases where two-parameter confidence contours intersect the $1/A_c = \eta = 0$ axis.

Several natural hazard examples that have previously been inferred to have power-law scaling were chosen to illustrate various effects of undersampling. Statistical analysis of data from the Miyako, Japan, tide gauge station that has a long historical catalog of tsunami events indicates that a Pareto distribution is well fit to the data. Estimates of β are close to one for this station, which is the limit where the statistical moments of a Pareto distribution are finite. For a tapered Pareto distribution, estimates of A_c appear to be

dependent on the estimates of β , indicating that joint two-parameter estimation methods should be employed for tsunamis. Although the power-law exponent β is little affected by the addition of a single extreme event (i.e., the 2011 Tohoku-oki tsunami), attempts to fit a tapered Pareto distribution with a corner parameter A_c are greatly affected by the addition of the 2011 Tohoku-oki tsunami measurement, indicating that the estimates of A_c are not stable with time. The upper confidence bound of A_c cannot be determined with or without the 2011 Tohoku-oki tsunami measurement.

Analysis of the Wenatchee and Arroyo Seco discharge catalogs in the United States illustrates the effects of climate on flood distributions (Turcotte and Haselton 1996). Partial duration floods along the Wenatchee River, which is in a maritime climate, closely follows a pure Pareto distribution with a relatively large value of β (> 2), such that the statistical moments are finite even without an exponential taper. In contrast, floods along the Arroyo Seco River appear to be best fit by a tapered Pareto distribution with a low value of β (≤ 1), though strictly speaking, the pure Pareto distribution cannot be ruled out with confidence. Like the tsunami example, estimates of β and A_c are jointly dependent.

For earthquakes, in contrast, the many orders of magnitude between the measurement threshold and largest events suggest that the estimates of β and A_c are approximately independent. Estimates for β are very well constrained by the catalog compared to other natural hazards. The MLE of β is less than one, indicating that the statistical moments of the pure Pareto distribution are infinite and suggesting that some taper must be physically required (Kagan 1999; Pisarenko and Sornette 2003). If one examines a sub-catalog of subduction zone earthquakes from 1982–2004, it appears that an upper bound for A_c can be confidently established, and that the pure Pareto null hypothesis can be rejected. However, that period of time is deficient in $m \geq 8.6$ earthquakes. In contrast, if one examines the full catalog that includes recent large-magnitude earthquakes, the confidence contours reach the $\eta = 0$ axis (null hypothesis cannot be rejected). Like the tsunami example, this indicates that the estimates of A_c are unstable with time.

The result A_c could be “determined” at high confidence with the 1982–2004 subduction zone earthquake catalog, whereas A_c is undefined for the 1982–2008 period illustrates a pitfall in hazard data selection. Aggregation of multiple catalogs increases the sample size, which conveys a sense of statistical power. However, stacking of independent and likely undersampled data sources is shown to produce an artificial Pareto taper that underestimates the true A_c value. This pitfall may apply to other natural hazards as well.

While it is reasonable to assume that the size of a natural hazard is physically limited or bounded, the available data often shed little light on the upper confidence bound for the corner size parameter for the hazard. Probabilistic hazard assessment methods can help determine limits on natural hazard size for a specified design probability, but these methods are dependent on information related to the size distribution of input parameters. Thus, the undersampling problem remains. Given that typically much more data would be need to be added to a catalog to determine confidence bounds on the corner size parameter, additional research in estimating the physical, theoretical limit of natural hazard size is the most likely way to address the problem of undersampling Pareto-distributed hazards.

Acknowledgments The authors would like to thank two anonymous reviewers for their highly constructive comments and Holly Ryan for reading an earlier version of this article.

References

- Aki K (1965) Maximum likelihood estimate of b in the formula $\log N = a - bM$ and its confidence limit. *Bull Earthq Res Inst* 43:237–239
- Andrews DJ, Hanks TC, Whitney JW (2007) Physical limits on ground motion at Yucca Mountain. *Bull Seismol Soc Am* 97:1771–1792
- Annaka T, Satake K, Sakakiyama T, Yanagisawa K, Shuto N (2007) Logic-tree approach for probabilistic tsunami hazard analysis and its applications to the Japanese Coasts. *Pure appl Geophys* 164:577–592
- Bird P (2003) An updated digital model of plate boundaries. *Geochem Geophys Geosyst* 4. doi:[10.1029/2001GC000252](https://doi.org/10.1029/2001GC000252)
- Bird P, Kagan YY (2004) Plate-tectonic analysis of shallow seismicity: apparent boundary width, beta-value, corner magnitude, coupled lithosphere thickness, and coupling in 7 tectonic settings. *Bull Seismol Soc Am* 94:2380–2399
- Bird P, Kagan YY, Jackson DD (2002) Plate tectonics and earthquake potential of spreading ridges and oceanic transform faults. In: Stein S, Freymueller JT (eds) *Plate boundary zones*. American Geophysical Union, Geodynamic Series, Washington, DC, pp 203–218
- Birkeland KW, Landry CC (2002) Power-laws and snow avalanches. *Geophys Res Lett* 29:49–41–49–43
- Burroughs SM, Tebbens SF (2001) Upper-truncated power laws in natural systems. *Pure appl Geophys* 158:741–757
- Burroughs SM, Tebbens SF (2005) Power law scaling and probabilistic forecasting of tsunami runup heights. *Pure appl Geophys* 162:331–342
- Chakrabarty A, Samorodnitsky G (2012) Understanding heavy tails in a bounded world or, is a truncated heavy tail heavy or not? *Stoch Models* 28:109–143
- Charnes A, Frome EL, Yu PL (1976) The equivalence of generalized least squares and maximum likelihood estimates in the exponential family. *J Am Stat As* 71:169–171
- Clauset A, Shalizi CR, Newman MEJ (2009) Power-law distributions in empirical data. *SIAM Rev* 51:661–703
- Cumming SG (2001) A parametric model of the fire-size distribution. *Can J For Res* 31:1297–1303
- Deemer WL, Votaw DF (1955) Estimation of parameters of truncated or censored exponential distributions. *Ann Math Stat* 26:498–504
- Dussauge C, Grasso JR, Helmstetter A (2003) Statistical analysis of rockfall volume distributions: implications for rockfall dynamics. *J Geophys Res* 108. doi:[10.1029/2001JB000650](https://doi.org/10.1029/2001JB000650)
- Fan J, Hung H-N, Wong W-H (2000) Geometric understanding of likelihood ratio statistics. *J Am Stat As* 95:836–841
- Field EH, Dawson TE, Felzer KR, Frankel AD, Gupta V, Jordan TH, Parsons T, Petersen MD, Stein RS, Weldon RJ, Wills CJ (2009) Uniform California earthquake rupture forecast, version 2 (UCERF 2). *Bull Seismol Soc Am* 99:2053–2107
- Flinn EA, Engdahl ER, Hill AR (1974) Seismic and geographical regionalization. *Bull Seismol Soc Am* 64:771–992
- Geist EL (2012) Phenomenology of tsunamis II: scaling, event statistics, and inter-event triggering. *Adv Geophys* 53:35–92
- Geist EL, Parsons T (2006) Probabilistic analysis of tsunami hazards. *Nat Hazards* 37:277–314
- Geist EL, Parsons T (2011) Assessing historical rate changes in global tsunami occurrence. *Geophys J Int* 187:497–509
- Geist EL, Parsons T, ten Brink US, Lee HJ (2009) Tsunami Probability. In: Bernard EN, Robinson AR (eds) *The sea*, vol 15. Harvard University Press, Cambridge, pp 93–135
- Grezio A, Marzocchi W, Sandri L, Gasparini P (2010) A Bayesian procedure for probabilistic Tsunami Hazard Assessment. *Nat Hazards* 53:159–174
- Gutenberg B, Richter CF (1944) Frequency of earthquakes in California. *Bull Seismol Soc Am* 34:185–188
- Hanks TC, Kanamori H (1979) A moment magnitude scale. *J Geophys Res* 84:2348–2350
- Hergarten S (2004) Aspects of risk assessment in power-law distributed natural hazards. *Nat Hazards Earth Syst Sci* 4:309–313
- Hergarten S, Neugebauer HJ (1998) Self-organized criticality in a landslide model. *Geophys Res Lett* 25:801–804
- Holschneider M, Zöller G, Hainzl S (2011) Estimation of the maximum possible magnitude in the framework of a doubly truncated Gutenberg–Richter model. *Bull Seismol Soc Am* 101:1649–1659
- Horikawa K, Shuto N (1983) Tsunami disasters and protection measures in Japan. In: Iida K, Iwasaki T (eds) *Tsunamis-their science and engineering*. Terra Scientific Publishing Company, Tokyo, pp 9–22
- Howell BF (1985) On the effect of too small a data base on earthquake frequency diagrams. *Bull Seismol Soc Am* 75:1205–1207

- IAEA (2011) Meteorological and Hydrological Hazards in Site Evaluation for Nuclear Installations. In: International Atomic Energy Agency, Vienna, p 172
- Ishimoto M, Iida K (1939) Observations of earthquakes registered with the microseismograph constructed recently. *Bull Earthq Res Inst* 17:443–478
- JSCE (2002) Tsunami assessment method for nuclear power plants in Japan. in: the tsunami evaluation subcommittee, the nuclear civil engineering committee, Japan Society of Civil Engineers, p 73
- Kagan YY (1993) Statistics of characteristic earthquakes. *Bull Seismol Soc Am* 83:7–24
- Kagan YY (1996) Comment on “The Gutenberg–Richter of characteristic earthquake distribution, which is it?” by Steven G. Wesnousky. *Bull Seismol Soc Am* 86:274–285
- Kagan YY (1999) Universality of the seismic-moment-frequency relation. *Pure appl Geophys* 155:537–573
- Kagan YY (2002) Seismic moment distribution revisited: I. Statistical results. *Geophys J Int* 148:520–541
- Kagan YY (2007) Earthquake size distribution and earthquake insurance. *Communications in statistics. Stoch Models* 13:775–797
- Kagan YY (2010) Earthquake size distribution: power-law with exponent $\beta = 1/2$? *Tectonophysics* 490:103–114
- Kagan YY, Jackson DD (2013) Tohoku earthquake: a surprise? *Bull Seismol Soc Am* 103:1181–1194
- Kagan YY, Schoenberg F (2001) Estimation of the upper cutoff parameter for the tapered Pareto distribution. *J Appl Probab* 38A:158–175
- Kagan YY, Bird P, Jackson DD (2010) Earthquake patterns in diverse tectonic zones of the globe. *Pure appl Geophys* 167:721–741
- Kidson R, Richards KS (2005) Flood frequency analysis: assumptions and alternatives. *Prog Phys Geogr* 29:392–410
- Kijko A (2004) Estimation of the maximum earthquake magnitude, m_{\max} . *Pure appl Geophys* 161:1655–1681
- Kijko A, Graham G (1998) Parametric-historic procedure for probabilistic seismic hazard analysis Part I: estimation of maximum regional magnitude m_{\max} . *Pure appl Geophys* 152:413–442
- Knopoff L, Kagan YY (1977) Analysis of the theory of extremes as applied to earthquake problems. *J Geophys Res* 82:5647–5657
- Korycansky DG, Lynett PJ (2005) Offshore breaking of impact tsunami: the Van Dorn effect revisited. *Geophys Res Lett* 32. doi:[10.1029/2004GL021918](https://doi.org/10.1029/2004GL021918)
- Kulikov EA, Rabinovich AB, Thomson R (2005) Estimation of tsunami risk for the coasts of Peru and northern Chile. *Nat Hazards* 35:185–209
- Lu ET, Hamilton RJ (1991) Avalanches and the distribution of solar flares. *Astrophys J* 380:L89–L92
- Lynett PJ, Wu T-R, Liu PL-F (2002) Modeling wave runup with depth-integrated equations. *Coast Eng* 46:89–107
- Main I (1996) Statistical physics, seismogenesis, and seismic hazard. *Rev Geophys* 34:433–462
- Main I, Li L, McCloskey J, Naylor M (2008) Effect of the Sumatran mega-earthquake on the global magnitude cut-off and event rate. *Nat Geosci* 1:142
- Main I, Naylor M, Greenhough J, Touati S, Bell AF, McCloskey J (2011) Model selection and uncertainty in earthquake hazard analysis. In: Faber M, Köhler J, Nishijima K (eds) *Applications of statistics and probability in civil engineering*. CRC Press, Leiden, pp 735–743
- Malamud BD, Turcotte DL (2006) The applicability of power-law frequency statistics to floods. *J Hydrol* 322:168–190
- Malamud BD, Turcotte DL, Barton CC (1996) The 1993 Mississippi River Flood: a one hundred or a one thousand year event? *Environ Eng Geosci* 2:479–486
- Malamud BD, Morein G, Turcotte DL (1998) Forest fires: an example of self-organized critical behaviour. *Science* 281:1840–1842
- Malamud BD, Turcotte DL, Guzzetti F, Reichenbach P (2004) Landslide inventories and their statistical properties. *Earth Surf Proc Land* 29:687–7111
- Marzocchi W, Newhall C, Woo G (2012) The scientific management of volcanic crises. *J Volcanol Geotherm Res* 247–248:181–189
- Mason BG, Pyle DM, Oppenheimer C (2004) The size and frequency of the largest explosive eruptions on earth. *Bull Volc* 66:735–748
- McCaffrey R (2008) Global frequency of magnitude 9 earthquakes. *Geology* 36:263–266
- Meerschaert MM, Roy P, Shao Q (2012) Parameter estimation for exponentially tempered power law distributions. *Commun Stat Theory Models* 41:1839–1856
- Mikhailov VN, Morozov VN, Cheroy NI, Mikhailova MV, Zav'yalova YF (2008) Extreme flood on the Danube River in 2006. *Russ Meteorol Hydrol* 33:48–54
- Nakamura S (1979) On statistics of tsunamis in Indonesia. *South East Asian Studies* 16:664–674

- Naylor M, Greenhough J, McCloskey J, Bell AF, Main IG (2009) Statistical evaluation of characteristic earthquakes in the frequency-magnitude distributions of Sumatra and other subduction zone regions. *Geophys Res Lett* 36. doi:[10.1029/2009GL040460](https://doi.org/10.1029/2009GL040460)
- Nelder JA, Mead R (1965) A simplex method for function minimization. *Comput J* 7:308–313
- Newman MEJ (2005) Power laws, Pareto distributions and Zipf's law. *Contemp Phys* 46:323–351
- Ozaki T (2011) Outline of the 2011 off the Pacific coast of Tohoku earthquake (Mw 9.0)–Tsunami warnings/ advisories and observations. *Earth Planets Space* 63:827–830
- Pacheco JF, Sykes LR (1992) Seismic moment catalog of large shallow earthquakes, 1900 to 1989. *Bull Seismol Soc Am* 82:1306–1349
- Parsons T, Geist EL (2009a) Is there a basis for preferring characteristic earthquakes over a Gutenberg–Richter distribution in probabilistic earthquake forecasting? *Bull Seismol Soc Am* 99:2012–2019
- Parsons T, Geist EL (2009b) Tsunami probability in the Caribbean region. *Pure appl Geophys* 165:2089–2116
- Parsons T, Console R, Falcone G, Murru M, Yamashina K (2012) Comparison of characteristic and Gutenberg–Richter models for time-dependent $M \geq 7.9$ earthquake probability in the Nankai–Tokai subduction zone, Japan. *Geophys J Int.* doi:[10.1111/j.1365-1246X.2012.05595.x](https://doi.org/10.1111/j.1365-1246X.2012.05595.x)
- Pisarenko VF, Sornette D (2003) Characterization of the frequency of extreme earthquake events by the Generalized Pareto Distribution. *Pure appl Geophys* 160:2343–2364
- Pisarenko VF, Sornette D (2004) Statistical detection and characterization of a deviation from the Gutenberg–Richter distribution above magnitude 8. *Pure appl Geophys* 161:839–864
- Porter K, Kennedy R, Bachman R (2007) Creating fragility functions for performance-based earthquake engineering. *Earthquake Spectra* 23:471–489
- Prasad R (2009) Tsunami hazard assessment at nuclear power plant sites in the United States of America. In: U.S. Nuclear Regulatory Commission, Washington DC, p 117
- Press WH, Teukolsky SA, Vetterling WT, Flannery BP (2007) Numerical recipes: the art of scientific computing. Cambridge University Press, Cambridge, p 1235
- Rabinovich AB, Stephenson FE (2004) Longwave measurements for the coast of British Columbia and improvements to the tsunami warning capability. *Nat Hazards* 32:313–343
- Rice JA (2007) Mathematical statistics and data analysis. Brooks/Cole, Cengage Learning, Belmont, p 672
- Rikitake T, Aida I (1988) Tsunami hazard probability in Japan. *Bull Seismol Soc Am* 78:1268–1278
- Sato H, Murakami H, Kozuki Y, Yamamoto N (2003) Study on a simplified method of tsunami risk assessment. *Nat Hazards* 29:325–340
- Schoenberg F, Peng R, Woods R (2003) On the distribution of wildfire sizes. *Environmetrics* 14:583–592
- Shuto N, Fujima K (2009) A short history of tsunami research and countermeasures in Japan. *Proc Jpn Acad Ser B* 85:267–275
- Soloviev SL (1970) Recurrence of tsunamis in the Pacific. In: Adams WM (ed) *Tsunamis in the Pacific Ocean*. East-West Center Press, Honolulu, pp 149–163
- Sornette D (2004) Critical phenomena in natural sciences. Springer, Berlin, p 528
- Sornette D, Sornette A (1999) General theory of the modified Gutenberg–Richter law for large seismic moments. *Bull Seismol Soc Am* 89:1121–1130
- Sornette D, Vanneste C, Sornette A (1991) Dispersion of b-values in Gutenberg–Richter Law as a consequence of a proposed fractal nature of continental faulting. *Geophys Res Lett* 18:897–900
- Stedinger JR, Vogel RM, Foufoula-Georgiou E (1993) Frequency analysis of extreme events. In: Maidment DR (ed) *Handbook of hydrology*. McGraw Hill, Inc., New York, pp 18.11–18.66
- Stein S, Newman A (2004) Characteristic and uncharacteristic earthquakes as possible artifacts: applications to the New Madrid and Wabash seismic zones. *Seismol Res Lett* 75:173–187
- Stein S, Geller RJ, Liu M (2012) Why earthquake hazard maps fail and what to do about it. *Tectonophys* 562–563:1–25
- Stern RJ (2002) Subduction zones. *Rev Geophys* 40. doi:[10.1029/2001RG000108](https://doi.org/10.1029/2001RG000108)
- Strauss D, Bednar L, Mees R (1989) Do one percent of the forest fires cause ninety-nine percent of the damage? *Forest Sci* 35:319–328
- ten Brink US, Geist EL, Andrews BD (2006) Size distribution of submarine landslides and its implication to tsunami hazard in Puerto Rico. *Geophys Res Lett* 33. doi:[10.1029/2006GL026125](https://doi.org/10.1029/2006GL026125)
- Turcotte DL, Green L (1993) A scale-invariant approach to flood-frequency analysis. *Stoch Hydrol Hydraul* 7:33–40
- Turcotte DL, Haselton K (1996) A dynamical systems approach to flood-frequency forecasting. In: Rundle JB, Turcotte DL, Klein W (eds) *Reduction and predictability of natural disasters*. Addison-Wesley, Reading, pp 51–70

- Utsu T (1999) Representation and analysis of the earthquake size distribution: a historical review and some new approaches. *Pure appl Geophys* 155:509–535
- Vere-Jones D, Robinson R, Yang W (2001) Remarks on the accelerated moment release model: problems of model formulation, simulation and estimation. *Geophys J Int* 144:517–531
- Wesnowsky SG (1994) The Gutenberg-Richter or characteristic earthquake distribution, which is it? *Bull Seismol Soc Am* 84:1940–1959
- Wyss M (1979) Estimating maximum expectable magnitude of earthquake from fault dimensions. *Geology* 6:336–340
- Yanagisawa K, Imamura F, Sakakiyama T, Annaka T, Takeda T, Shuto N (2007) Tsunami assessment of risk management at nuclear power facilities in Japan. *Pure appl Geophys* 164:565–576
- Yen BC (1988) Flood hazards for nuclear power plants. *Nucl Eng Des* 110:213–219
- Zaliapin IV, Kagan YY, Schoenberg FP (2005) Approximating the distributions of Pareto sums. *Pure appl Geophys* 162:1187–1228
- Zöller G (2013) Convergence of the frequency-magnitude distribution of global earthquakes: maybe in 200 years. *Geophys Res Lett* 40:3873–3877